

# First principle calculations of $XAl_3$ ( $X= Sc, Ti, Fe, Ni, Y, Zr$ and $Ta$ ) compounds: elastic and thermodynamic properties

DU XIAOMING<sup>a,\*</sup>, LIU FENGGU<sup>a</sup>, LI JING<sup>b</sup>, WU ERDONG<sup>b</sup>

<sup>a</sup>*School of Materials Science and Engineering, Shenyang Ligong University, Shenyang 110159, China*

<sup>b</sup>*Institute of Metal Research, Chinese Academy of Sciences, Shenyang 110016, China*

Elastic and thermodynamic properties of the  $XAl_3$  ( $X= Sc, Ti, Fe, Ni, Y, Zr$  and  $Ta$ ) intermetallic compounds were investigated by means of first-principles calculations within the framework of density functional theory. The single-crystal elastic constants were calculated, showing that the  $XAl_3$  intermetallic compounds are mechanically stable structure. Then the bulk modulus  $B$ , Young's modulus  $E$ , shear modulus  $G$  and Poisson's ratio  $\nu$  were estimated for polycrystalline  $Al_3X$  from the elastic constants by the Voigt–Reuss–Hill (VRH) approximation. The ductility of  $XAl_3$  intermetallic compounds was analyzed, and  $FeAl_3$  and  $ZrAl_3$  compounds are ductile. The elastic anisotropy was also further discussed in details. Finally, thermodynamic properties such as the Debye temperatures, the specific heat for the  $XAl_3$  intermetallic compounds were estimated from elastic properties.

(Received November 30, 2014; accepted May 7, 2015)

*Keywords:* Trialuminide intermetallic compounds, First-principles calculations, Elastic properties, Thermodynamic properties

## 1. Introduction

The trialuminide intermetallic compounds with transition metals ( $Sc, Ti, Zr, Y, Fe, Ni$  and  $Ta$ ) usually exhibit one or more of the three ordered structures: cubic- $L1_2$ , or tetragonal- $DO_{22}$  or orthorhombic structures [1]. The phase stability of cubic  $L1_2$ -structured trialuminides is of fundamental importance for its use in at least two applications: (i) as potential high-temperature structural materials, and (ii) for the design of high-temperature, creep-resistant aluminum-based alloys containing coherent precipitates [1]. Related to (ii), among binary alloy systems  $Al-Sc$  exhibits nanoscale precipitates of coherent  $L1_2-Al_3Sc$  as an equilibrium phase in an  $(Al)$  matrix [2,3]. However  $L1_2$ -structural  $Al_3Sc$  is brittle at room temperature which was caused by an insufficient number of slip system and poor grain boundary cohesion [4]. In despite of it,  $Al_3Sc$  is very significant in providing super plastic ductility to  $Al$  based alloys [5-7]. In addition, similar to  $Sc$ , what would the effect of  $Ti, Zr, Y, Fe, Ni$  and  $Ta$  transition metals on elastic and thermodynamic properties of  $Al$  based alloys be expected? How does the polycrystalline materials exhibit their mechanical properties?

Elastic properties provide information about the interatomic bounding strength and its anisotropy, the criterion of structural stability, the measurement of lattice vibrations of acoustic modes, the correlation from an atomistic theory to a macroscopic material model, as well as the indications of ductility/brittleness, hardness, melting points, etc. Recently, Shang et al. [8] systematically studied the elastic properties of pure elements with bcc,

fcc and hcp structures. Ganeshan et al. [9] constructed an elastic property database of binary  $Mg$  compounds from first-principles calculations.

In the present work, first-principles calculations were employed to predict the elastic and thermodynamic properties for binary  $XAl_3$  ( $X= Sc, Ti, Fe, Ni, Y, Zr$  and  $Ta$ ) intermetallic compounds. They consist of elastic constants  $C_{ij}$ , Young's modulus  $E$ , shear modulus  $G$ , bulk modulus  $B$ , Poisson's ratio  $\nu$ , anisotropy indexes  $A$ . Based on the calculated elastic constants and modulus, the Debye temperature and the specific heat are also investigated.

## 2. Computational method

All calculations were performed by using the first principle calculations based on density functional theory (DFT) [10] implemented in Quantum-ESPRESSO program package [11]. Meanwhile, the exchange and correlation energies were calculated with in the generalized gradient approximation of Perdew-Wang91 version (GGA-PW91). The Monkhorst-Pack scheme [12] was used for  $k$  point sampling in the first irreducible Brillouin zone (BZ). The  $k$  points separation in the Brillouin zone of the reciprocal space were  $18 \times 18 \times 18$ ,  $12 \times 12 \times 6$ ,  $14 \times 4 \times 12$ ,  $15 \times 12 \times 18$ ,  $18 \times 18 \times 18$ ,  $18 \times 18 \times 18$  and  $12 \times 12 \times 6$  for  $ScAl_3$ ,  $TiAl_3$ ,  $FeAl_3$ ,  $NiAl_3$ ,  $YAl_3$ ,  $ZrAl_3$ ,  $TaAl_3$ , respectively. The cutoff energy for plane wave expansions was determined as 540 eV after convergence tests. The convergence criteria for geometry optimization was as follows: electronic self-consistent field (SCF) tolerance less than  $5.0 \times 10^{-5}$  eV/atom, Hellmann–Feynman force below  $0.01 \text{ eV}/\text{\AA}$ , maximum stress less than  $0.05 \text{ GPa}$

and displacement within  $2.0 \times 10^{-4}$  Å. The crystal structures of seven stable  $XAl_3$  ( $X= Sc, Ti, Fe, Ni, Y, Zr$  and  $Ta$ ) intermetallic compounds are shown in Fig. 1. The lattice parameters are tabulated in Table 1.

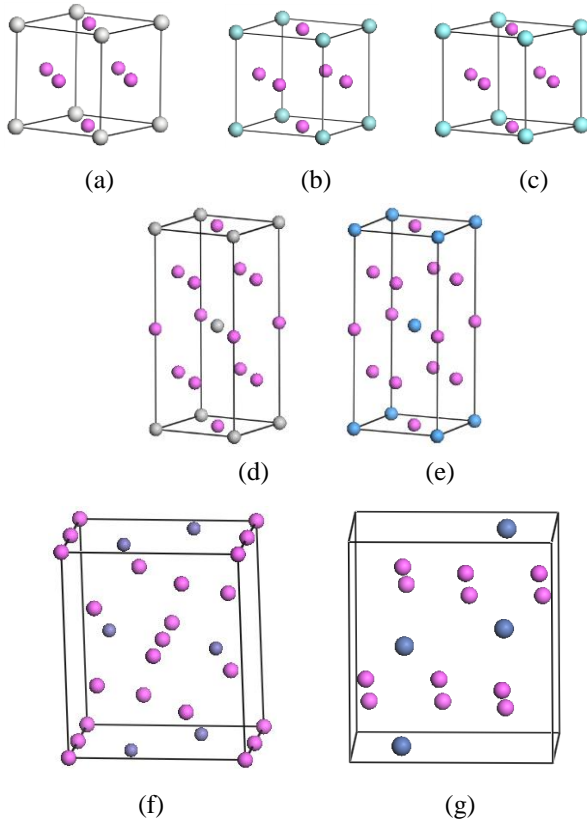


Fig. 1. The crystal structures of  $XAl_3$  ( $X= Sc, Ti, Fe, Ni, Y, Zr$  and  $Ta$ ) intermetallic compounds, (a)  $ScAl_3$ , (b)  $ZrAl_3$ , (c)  $YAl_3$ , (d)  $TiAl_3$ , (e)  $TaAl_3$ , (f)  $FeAl_3$  and (g)  $NiAl_3$ . The purple balls represent Al and other balls represent transition metal atoms.

### 3. Results and discussions

#### 3.1 Crystal structures

In present work, the original crystal structures have been built based upon the experimental crystallographic data of seven stable  $XAl_3$  ( $X= Sc, Ti, Fe, Ni, Y, Zr$  and  $Ta$ ) intermetallic compounds [13-19]. Starting from the above crystal structure, the structural optimization was first performed by full relaxation of cell shape and atomic positions. The optimized lattice parameters are listed in Table 1, where the available experimental results are also presented. The maximum deviation between the experiments and the calculated values is less 1.4%. The calculated lattice parameters of  $XAl_3$  ( $X= Sc, Ti, Fe, Ni, Y, Zr$  and  $Ta$ ) intermetallic compounds agree very well with the available experimental data. These agreements of optimized lattice parameters with the experimental values provide a confirmation that the computational methodology used in this work is suitable and reliable.

#### 3.2 Elastic constants and mechanical stability

The single-crystal elastic constants can be obtained by applying a small strain to the equilibrium lattice and computing the resultant change in its total energy [20, 21]. To calculate the elastic constants

$C_{ij}$ , a deformed cell is introduced. The elastic strain energy is given by following [22]:

$$U = E - E_0 = \frac{V_0}{2} \sum_{i=1}^6 \sum_{j=1}^6 C_{ij} \varepsilon_i \varepsilon_j + O(\varepsilon^3) \quad (1)$$

where  $E$  and  $E_0$  are the total energies of the distorted and equilibrium structures, respectively.  $V_0$  is the equilibrium volume.  $\varepsilon_i$  and  $\varepsilon_j$  are strain.

Table 1. Calculated and experimental lattice parameters for  $XAl_3$  ( $X= Sc, Ti, Fe, Ni, Y, Zr$  and  $Ta$ ) intermetallic compounds.

Alloys	Space group	Pearson symbol	Lattice parameters (Å)			Refs.
			a	b	c	
$ScAl_3$	$Pm-3m$	cP4	4.109			Present
			4.101			
$TiAl_3$	$I4/mmm$	tI8	3.852	3.852	8.614	Present
			3.854	3.854	8.584	
$FeAl_3$	$Cmcm$	oS24	7.555	6.389	4.304	Present
			7.656	6.415	4.218	
$NiAl_3$	$Pnma$	oP16	6.690	7.377	4.787	Present
			6.598	7.352	4.802	
$YAl_3$	$Pm-3m$	cP4	4.278			Present
			4.323			
$ZrAl_3$	$Pm-3m$	cP4	4.110			Present
			4.093			
$TaAl_3$	$I4/mmm$	tI8	3.862	3.862	8.599	Present
			3.841	3.841	8.537	

The calculated elastic constants  $C_{ij}$  of the  $XAl_3$  ( $X=Sc, Ti, Fe, Ni, Y, Zr$  and  $Ta$ ) intermetallic compounds together with the available experimental and theoretical data [23-26] are listed in Table 2. The calculated elastic constants of these compounds are in good agreement with the available reported data. The intrinsic mechanical stability of a solid is in general determined by certain conditions related to the crystal symmetry. The mechanical stabilities of the seven compounds have been analyzed according to elastic constants. For different crystals, the elastic constants need to satisfy the generalized stability criteria:  $C_{11} > 0$ ,  $C_{44} > 0$ ,  $C_{11} > C_{12}$ ,  $C_{11} + 2C_{12} > 0$  for cubic

crystals [27];  $C_{11} > 0$ ,  $C_{33} > 0$ ,  $C_{44} > 0$ ,  $C_{66} > 0$ ,  $C_{11} > C_{12}$ ,  $C_{11} + C_{33} - 2C_{13} > 0$ ,  $2C_{11} + C_{33} + 2C_{12} + 4C_{13} > 0$  for tetragonal crystals [28];  $C_{11} > 0$ ,  $C_{22} > 0$ ,  $C_{33} > 0$ ,  $C_{44} > 0$ ,  $C_{55} > 0$ ,  $C_{66} > 0$ ,  $C_{11} + C_{22} - 2C_{12} > 0$ ,  $C_{11} + C_{33} - 2C_{13} > 0$ ,  $C_{22} + C_{33} - 2C_{23} > 0$ ,  $C_{11} + C_{22} + C_{33} + 2C_{12} + 2C_{13} + 2C_{23} > 0$  for orthorhombic crystals [29]. It is obvious that, from Table 2, all the elastic constants of the three cubic crystals ( $ScAl_3$ ,  $YAl_3$  and  $ZrAl_3$ ), the two tetragonal crystals ( $TiAl_3$  and  $TaAl_3$ ) and two orthorhombic crystals ( $FeAl_3$  and  $NiAl_3$ ) meet the corresponding crystal's mechanical stability criteria. The results reveal that all the seven  $XAl_3$  intermetallic compounds are mechanically stable.

Table 2. The calculated elastic constants,  $C_{ij}$  (in GPa) for  $XAl_3$  ( $X=Sc, Ti, Fe, Ni, Y, Zr$  and  $Ta$ ) intermetallic compounds (present study) with the available reported data.

Alloys	$C_{11}$	$C_{12}$	$C_{13}$	$C_{22}$	$C_{23}$	$C_{33}$	$C_{44}$	$C_{55}$	$C_{66}$
$ScAl_3$	154.17	75.34					161.90		
$TiAl_3$	176.50	93.6	43.9			218.81	79.84		131.75
	182 <sup>a</sup>	92 <sup>a</sup>	42 <sup>a</sup>			215 <sup>a</sup>	88 <sup>a</sup>		125 <sup>a</sup>
	192 <sup>b</sup>	84 <sup>b</sup>	49 <sup>b</sup>			216 <sup>b</sup>	94 <sup>b</sup>		122 <sup>b</sup>
$FeAl_3$	185.98	111.29	114.59	322.07	-16.01	233.64	93.30	28.44	53.48
$NiAl_3$	180.71	53.52	42.67	216.06	61.94	307.18	115.39	60.57	105.54
	188.1 <sup>c</sup>	80.6 <sup>c</sup>	75.3 <sup>c</sup>	195.3 <sup>c</sup>	69 <sup>c</sup>	186.2 <sup>c</sup>	84.7 <sup>c</sup>	64.9 <sup>c</sup>	67.8 <sup>c</sup>
	169 <sup>d</sup>	87 <sup>d</sup>	94 <sup>d</sup>	167 <sup>d</sup>	81 <sup>d</sup>	164 <sup>d</sup>	89 <sup>d</sup>	74 <sup>d</sup>	51 <sup>d</sup>
$YAl_3$	150.20	70.48					143.7		
$ZrAl_3$	125.29	116.73					126.26		19.75
$TaAl_3$	249.14	71.26	11.63			166.14	145.72		2.59

<sup>a</sup> Ref. [23].

<sup>b</sup> Ref. [24].

<sup>c</sup> Ref. [25].

<sup>d</sup> Ref. [26].

### 3.3 Elastic properties for polycrystalline aggregates

The elastic properties of polycrystalline materials are usually characterized by the elastic moduli, such as bulk modulus ( $B$ ), Young's modulus ( $E$ ), shear modulus ( $G$ ) and Poisson ratio  $\nu$ . On the basis of the approximations by Voigt [30] and Reuss [31] and Hill's empirical average [32], we have calculated the corresponding bulk moduli  $B=(B_V+B_R)/2$  and shear moduli  $G=(G_V+G_R)/2$  (where the subscripts V and R refer to the Voigt and Reuss bounds, respectively.) which are listed in Table 3 along with the experimental and other theoretical values [23-26]. Additionally the Young's modulus  $E$  and Poisson ratio  $\nu$  have been calculated using Hill's empirical average and the equations:

$$E = 9BG / (3B + G) \quad (2)$$

and

$$\nu = (3B - 2G) / (6B + 2G) \quad (3)$$

The bulk modulus  $B$  can be used as a measure of the average bond strength of atoms for the given crystal. As listed in Table 3,  $FeAl_3$  has the highest bulk modulus (127.13 GPa), while  $TaAl_3$  possesses the lowest one (91.10 GPa). Therefore,  $FeAl_3$  has the strongest average bond strength of atoms and  $TaAl_3$  has the lowest one. The shear modulus is the relationship between the resistance to reversible deformations and the shear stress. The ratio of the bulk modulus  $B$  to shear modulus  $G$  of the compounds, proposed by Pugh [34], can empirically predict the brittle and ductile behavior of materials. The compound with smaller  $B/G$  value ( $<1.75$ ) usually is brittle while the compound with larger  $B/G$  value ( $>1.75$ ) is ductile. The  $B/G$  values of  $FeAl_3$  and  $ZrAl_3$  compounds larger than

1.75 (Table 3) suggests that the two compounds are ductile. Whileas the other compounds here are brittle with their values of  $B/G$  smaller than 1.75. As another elastic parameter of compounds, Poisson's ratio  $\nu$  is consistent with  $B/G$ , which refers to ductile compounds usually with a large  $\nu$  ( $>0.26$ ) [35]. The values of values of  $\nu$  are larger than 0.26 for  $FeAl_3$  and  $ZrAl_3$  compounds in Table 3, which indicates that these two compounds are ductile. However,  $B/G$  and Poisson's ratios of the two ductile  $FeAl_3$  and  $ZrAl_3$  compounds are still less than pure Al and Zr (Table 3), equally indicating that these intermetallics in  $XAl_3$  system are relatively brittle and will reduce the ductility of X-Al alloys.

Besides,  $C_{11}$ - $C_{12}$  and Young's modulus  $E$  are other two significant indications of the mechanical properties of

materials. The Young's modulus is defined as the ratio of stress and strain and can also be used as a measure of the stiffness of a solid. When the value of Young's modulus is large, the material is stiff. In the present work,  $ScAl_3$  is stiffest of the considered compounds due to its highest value of Young's modulus (212.97 GPa). The smaller values of  $C_{11}$ - $C_{12}$  and Young's modulus  $E$  correspond to the better plasticity of materials. In order to get an intuitive knowledge for the plasticity of the  $XAl_3$  intermetallic compounds, the calculated results of the  $XAl_3$  intermetallic compounds are shown in Fig. 2. From the results in Tables 3 and Fig. 2, it can be seen that  $ZrAl_3$  has lowest values of  $C_{11}$ - $C_{12}$  and Young's modulus  $E$ , implying the greatest plasticity.

Table 3. The calculated bulk modulus  $B$  (GPa), shear modulus  $G$  (GPa), Young's modulus  $E$  (GPa),  $B/G$ , Poisson's ratio  $\nu$ , anisotropic index  $A^U$  for  $XAl_3$  intermetallic compounds.

Alloys	$B$	$G$	$E$	$B/G$	$\nu$	$B_V/B_R$	$G_V/G_R$	$A^U$
$ScAl_3$	101.62	92.54	212.97	1.098	0.151	1.000	1.564	2.82
$TiAl_3$	103.83	78.9	188.86	1.316	0.197	1.000	1.147	0.735
	103 <sup>a</sup>	83 <sup>a</sup>	196 <sup>a</sup>	1.25 <sup>a</sup>	0.18 <sup>a</sup>			
	107 <sup>b</sup>	89 <sup>b</sup>	199 <sup>b</sup>	1.19 <sup>b</sup>	0.18 <sup>b</sup>			
$FeAl_3$	127.13	58.64	152.48	2.168	0.30	1.031	1.507	2.566
$NiAl_3$	110.84	89.40	211.37	1.240	0.182	1.047	1.706	0.427
	113.2 <sup>c</sup>	65.7 <sup>c</sup>	165.2 <sup>c</sup>	1.72 <sup>c</sup>				0.113 <sup>c</sup>
	113 <sup>d</sup>							
$YAl_3$	97.05	86.23	199.58	1.125	0.157	1.000	1.452	2.260
$ZrAl_3$	119.58	49.86	131.33	2.398	0.317	1.000	8.720	38.60
$TaAl_3$	91.10	54.32	135.94	1.677	0.251	1.085	8.20	36.10
Al				2.89 <sup>e</sup>	0.35 <sup>e</sup>			
$\alpha$ -Zr				2.50 <sup>e</sup>	0.32 <sup>e</sup>			

<sup>a</sup> Ref. [23].

<sup>b</sup> Ref. [24].

<sup>c</sup> Ref. [25].

<sup>d</sup> Ref. [26].

<sup>e</sup> Ref. [33].

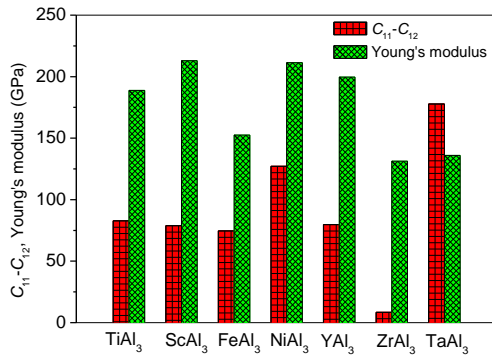


Fig. 2. The values of  $C_{11}$ - $C_{12}$  and Young's modulus for  $XAl_3$  intermetallic compounds.

### 3.4 Elastic anisotropy

The elastic constants of solids are very important because they are closely associated with the mechanical and physical properties. In particular, they play an important part in providing valuable information about structural stability and anisotropic characteristics.

The universal elastic anisotropy index  $A^U$  for crystals with any symmetry is proposed as follow [36]:

$$A^U = 5 \frac{G_V}{G_R} + \frac{B_V}{B_R} - 6 \geq 0 \quad (4)$$

where  $B_V$  ( $G_V$ ) and  $B_R$  ( $G_R$ ) are the bulk modulus (shear modulus) in the Voigt and Reuss approximations. A crystal with  $A^U = 0$  means it is isotropic. The deviation of  $A^U$  from zero defines the extent of single crystal anisotropy ( i. e. the larger  $A^U$  represents the more anisotropic) and

accounts for both the shear and the bulk contributions unlike all other existing anisotropy measures. Obviously, the increase in the  $G_V/G_R$  affects the anisotropy  $A^U$  much more than in  $B_V/B_R$  because of the coefficient for  $G_V/G_R$  ( $=5$ ) larger than that for  $B_V/B_R$  ( $=1$ ). The values of  $A^U$  for seven  $XAl_3$  compounds are listed in Table 3. For cubic structures  $ZrAl_3$ ,  $ScAl_3$  and  $YAl_3$ , although their values of  $B_V/B_R$  are the same, the  $G_V/G_R$  for  $ZrAl_3$  is 8.72 which is the largest in these three compounds. Therefore,  $ZrAl_3$  is the most anisotropic, followed by  $ScAl_3$  and by  $YAl_3$ . We can deduce the similar conclusions for tetragonal structures ( $TiAl_3$  and  $TaAl_3$ ) and orthorhombic structures ( $FeAl_3$  and  $NiAl_3$ ). It should be noted that the cubic  $ZrAl_3$  with the largest  $A^U = 38.6$  is the most anisotropic in  $XAl_3$  compounds.

The elastic anisotropy of crystal is closely correlated with the possibility to induce microcracks and dislocations in the materials [37,38]. The shear resistance of crystal (the energy change in a crystal associated with the shear modes along different slip directions) is characterized by the elastic anisotropy factors. In the cubic crystal, the anisotropic behavior can be described by one shear factor:  $A_1=2C_{44}/(C_{11}-C_{12})$  for the  $\{100\}$  shear planes in  $\langle 010 \rangle$  and  $\langle 110 \rangle$  directions. In the tetragonal crystal, the

anisotropic behavior can be described by three shear factors:  $A_1=2C_{66}/(C_{11}-C_{12})$ ,  $A_2=4C_{44}/(C_{11}+C_{33}-2C_{13})$  and  $A_3=C_{44}/C_{66}$ . They are corresponding to the  $\{001\}$  shear plane along the  $\langle 010 \rangle$  direction, the  $\{011\}$  shear plane along the  $\langle 011 \rangle$  direction and  $\{100\}$  shear plane along the  $\langle 100 \rangle$  direction, respectively. For orthorhombic crystal, the anisotropic behavior can be described by three shear factors:  $A_1=4C_{44}/(C_{11}+C_{33}-2C_{13})$ ,  $A_2=2C_{55}/(C_{22}+C_{33}-2C_{23})$ , and  $A_3=4C_{66}/(C_{11}+C_{22}-2C_{12})$ . They are corresponding to the  $\{100\}$  shear planes between  $\langle 010 \rangle$  and  $\langle 011 \rangle$  directions, the  $\{010\}$  shear planes between  $\langle 001 \rangle$  and  $\langle 101 \rangle$  directions and the  $\{001\}$  shear planes between  $\langle 010 \rangle$  and  $\langle 110 \rangle$  directions, respectively. For an isotropic crystal the factors  $A_1$ ,  $A_2$  and  $A_3$  must be unity. The deviation of the anisotropic factors from unity is a measure for the elastic anisotropy. The calculated values of the elastic anisotropy factors for seven  $Al_3X$  intermetallic compounds listed in Table 4 show that all elastic anisotropy factors go towards unity. It should be noted that the cubic  $ZrAl_3$  with the largest  $A_1 = 29.5$  and the tetragonal  $TaAl_3$  with the largest  $A_3 = 56.3$  is the most anisotropic in cubic and tetragonal structures, respectively.

Table 4. Elastic anisotropy ratios  $A_1$ ,  $A_2$ , and  $A_3$  for  $XAl_3$  intermetallic compounds.

	$ScAl_3$	$TiAl_3$	$FeAl_3$	$NiAl_3$	$YAl_3$	$ZrAl_3$	$TaAl_3$
$A_1$	4.11	3.18	1.96	1.15	3.61	29.5	0.029
$A_2$		1.04	0.19	0.61			1.49
$A_3$		0.61	0.75	1.46			56.3

According to the calculated elastic constants, we can obtain the directional dependence of the Young's modulus for the  $XAl_3$  intermetallic compounds, and it can be expressed as [39]:

For the cubic symmetry crystal,

$$\frac{1}{E} = S_{11} - 2(S_{11} - S_{12} - \frac{1}{2}S_{44})(l_1^2l_2^2 + l_1^2l_3^2 + l_2^2l_3^2) \quad (5)$$

For the tetragonal symmetry crystal,

$$\frac{1}{E} = S_{11}(l_1^4 + l_2^4) + S_{33}l_3^4 + (2S_{12} + S_{66})l_1^2l_2^2 + l_3^2(1-l_3^2)(2S_{13} + S_{44}) \quad (6)$$

For the orthorhombic symmetry crystal,

$$\frac{1}{E} = S_{11}l_1^4 + S_{22}l_2^4 + S_{33}l_3^4 + (2S_{12} + S_{66})l_1^2l_2^2 + l_3^2(2S_{33} + S_{44}) + l_1^2l_3^2(2S_{13} + S_{55}) \quad (7)$$

where  $l_1$ ,  $l_2$ , and  $l_3$  are the directional cosines, and they can

be obtained by  $l_1=\sin[\theta]\cos[\varphi]$ ,  $l_2=\sin[\theta]\sin[\varphi]$  and  $l_3=\cos[\theta]$  in spherical coordinates. The angles  $\theta$  and  $\varphi$  are well defined in spherical coordinates.  $S_{ij}$  is defined as an elastic compliance matrix. Then, the directional dependence of Young's modulus can be obtained from calculated compliance constants and direction cosine, and the results are shown in Fig. 3. For an isotropic system, the directional dependence of Young's modulus should be spherical shape. As can be seen from Fig. 3, the Young's modulus graphs for  $XAl_3$  intermetallic compounds clearly show nonspherical shape, which indicates that the Young's modulus of these compounds are anisotropic. For cubic structures,  $ScAl_3$  and  $ZrAl_3$  compounds have strong anisotropy in  $\langle 100 \rangle$  crystal direction. The anisotropy of  $TaAl_3$  is stronger than that of  $TiAl_3$  in tetragonal symmetry crystal. This large elastic anisotropy is considered to be closely related to the interatomic bonding strength. It is noted that  $TaAl_3$  and  $ZrAl_3$  show the strongest anisotropy of seven  $XAl_3$  compounds. This agrees with the analyses of elastic anisotropy index  $A^U$  in Table 3 and elastic anisotropy ratios  $A_1$ ,  $A_2$ , and  $A_3$  in Table 4.

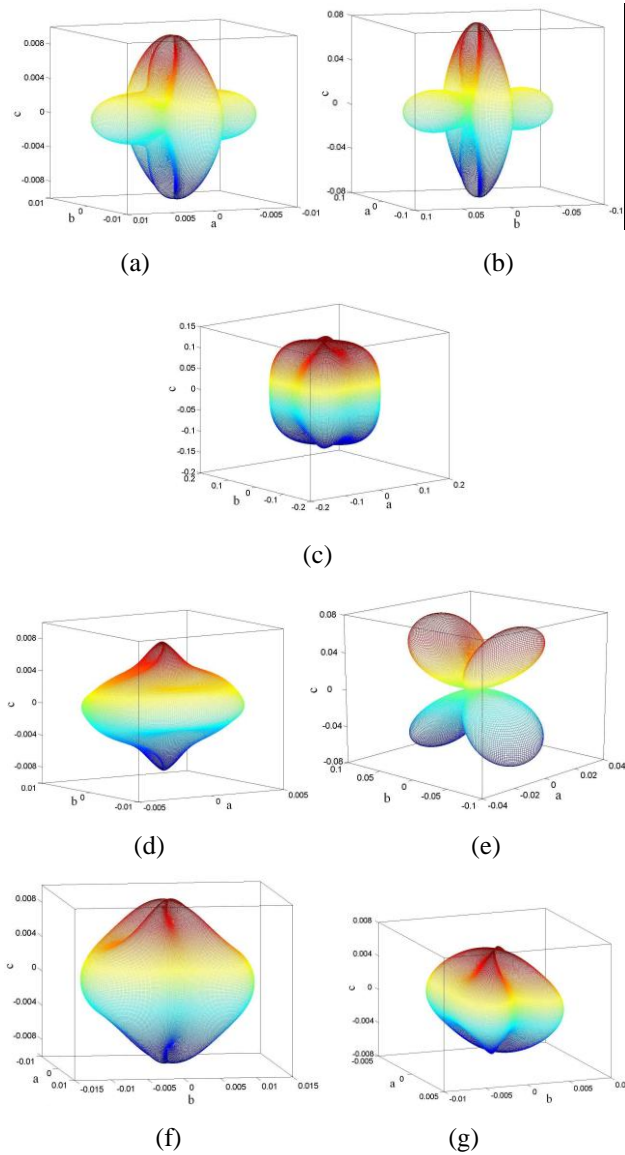


Fig. 3. Directional dependence of Young's modulus in  $XAl_3$  intermetallic compounds, (a)  $ScAl_3$ , (b)  $ZrAl_3$ , (c)  $YAl_3$ , (d)  $TiAl_3$ , (e)  $TaAl_3$ , (f)  $FeAl_3$ , (g)  $NiAl_3$ .

### 3.5 Thermodynamic properties

The Debye temperature  $\theta_D$  is a fundamental attribute of a solid connecting elastic properties with thermodynamic properties such as specific heat, sound velocity and melting temperature. It can be calculated from the averaged sound velocity,  $v_m$  by the following equation [40]:

$$\theta_D = \frac{h}{k_B} \left[ \frac{3n}{4\pi} \left( \frac{N_A \rho}{M} \right) \right]^{\frac{1}{3}} v_m \quad (8)$$

where  $h$  is Planck's constant,  $k_B$  is Boltzmann's constant,  $N_A$  is Avogadro's number,  $n$  is the number of atoms in the unit cell,  $M$  is the molecular weight and  $\rho$  is the density. The average sound velocity in the polycrystalline material is approximately given by [40]:

$$v_m = \left[ \frac{1}{3} \left( \frac{2}{v_s^3} + \frac{1}{v_l^3} \right) \right]^{-1/3} \quad (9)$$

where  $v_l$  and  $v_s$  are the longitudinal and transverse sound velocity, respectively, which can be obtained using the shear modulus  $G$  and the bulk modulus  $B$  from Navier's equations [41]:

$$v_l = \sqrt{\frac{B + 4G/3}{\rho}} \quad \text{and} \quad v_s = \sqrt{\frac{G}{\rho}} \quad (10)$$

The calculated values of sound velocity and Debye temperature as well as the density for the seven  $XAl_3$  compounds are given in Table 5. There are no clear trends that can be observed from the data in Table 5 for the  $XAl_3$  compounds. However,  $ScAl_3$  has a highest Debye temperature in the considered  $XAl_3$  compounds in this study. As a rule of thumb, a higher Debye temperature means a larger associated thermal conductivity [42]. Therefore,  $ScAl_3$  should possess the best thermal conductivity relative to the other  $XAl_3$  compounds.

In the approximation of Debye model, the specific heat of the solid,  $C_v$  can be obtained from Debye temperature by the following equation [43]

$$C_v = 9N_A k_B (T / \theta_D)^3 \int_0^{\theta_D/T} \frac{x^4 e^x}{(e^x - 1)^2} dx \quad (11)$$

where  $T$  is the temperature (K).

The calculated values of the specific heat of seven  $XAl_3$  intermetallic compounds the are shown in Fig. 4. The specific heat of these intermetallic compounds is similar and increases with increasing temperature below  $\theta_D$ . However, the specific heat of these compounds is gradually close to 25 J/mol·K for the high temperature case ( $T \gg \theta_D$ ), which is the Dulong-Petit result (equal to  $3N_A k_B$ ) from classical thermodynamics. For low temperature case ( $T \ll \theta_D$ ), the electron specific heat becomes significant for metals and is combined with the above specific heat in the Einstein-Debye specific heat [44].

Table 5. The calculated density ( $\rho$ ), the longitudinal, transverse, and average sound velocity ( $v_l$ ,  $v_s$ ,  $v_m$ ), the Debye temperatures ( $\theta_D$ ) and the melting temperature ( $T_m$ ).

Compounds	$v_l$ (m·s <sup>-1</sup> )	$v_s$ (m·s <sup>-1</sup> )	$v_m$ (m·s <sup>-1</sup> )	$\rho$ (kg·m <sup>-3</sup> )	$\theta_D$ (K)
ScAl <sub>3</sub>	7326	5538	5940	3017	683
TiAl <sub>3</sub>	6414	4849	5200	3356	615
FeAl <sub>3</sub>	4999	3779	4052	4106	503
NiAl <sub>3</sub>	6310	4770	5116	3929	621
ZrAl <sub>3</sub>	4601	3478	3730	4122	429
YAl <sub>3</sub>	6471	4891	5246	3604	580
TaAl <sub>3</sub>	3743	2830	3035	6784	358

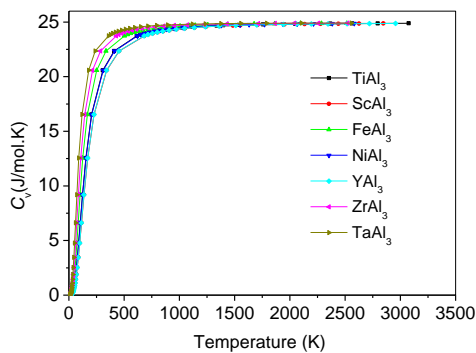


Fig. 4. The dependence of specific heat on temperature for XAl<sub>3</sub> intermetallic compounds.

#### 4. Conclusions

In summary, we have calculated and analyzed the elastic properties of the XAl<sub>3</sub> (X= Sc, Ti, Fe, Ni, Y, Zr and Ta) intermetallic compounds by the plane-wave ultrasoft pseudopotential method based on the density-functional theory. We have also calculated the shear modulus,  $G$ ; Young's modulus,  $E$ ; and Poisson's ratio  $\nu$  for ideal polycrystalline XAl<sub>3</sub> aggregates within the scheme of Voigt–Reuss–Hill (VRH) approximation, and the ductility was then analyzed. The elastic anisotropy was also discussed in details. The results show that XAl<sub>3</sub> (X= Sc, Ti, Fe, Ni, Y, Zr and Ta) intermetallic compounds are mechanically stable structures. FeAl<sub>3</sub> and ZrAl<sub>3</sub> compounds are ductile. And ScAl<sub>3</sub> possesses the highest stiffness due to its highest values of Young's modulus and  $C_{11}$ - $C_{12}$ . The calculated results of the anisotropic indexes of single crystal show that all XAl<sub>3</sub> compounds are anisotropic. The cubic ZrAl<sub>3</sub> with the largest  $A^U = 38.6$  is the most anisotropic in XAl<sub>3</sub> compounds. Finally, we have derived thermodynamic properties such as the sound velocity, the Debye temperatures and the specific heat for the XAl<sub>3</sub> compounds.

#### Acknowledgement

The authors gratefully acknowledge the financial support by the program for Shenyang Ligong University Key Laboratory Opening Fund in advanced materials processing technology in Liaoning Province, China.

#### References

- [1] G. Ghosh, A. van de Walle, M. Asta, J. Phase Equilib. Diff. **28**, 9 (2007).
- [2] M. Y. Drita, L. B. Ber, Y. G. Bykov, L. S. Toropova, G. K. Anastasyeva, Fiz. Met. Metallov. **57**, 1172 (1984).
- [3] D. N. Seidman, E. A. Marquis, D. C. Dunand, Acta Mater. **50**, 4021 (2002).
- [4] C. Liu, J. Stiegler, Science **226**, 636 (1984).
- [5] H. B. Hyde, A. F. Norman, R. B. Prangnell, Acta Mater. **49**, 1327 (2001).
- [6] S. Lee, A. Utsunomiya, H. Akamatsu, K. Neishi, M. Furukawa, Z. Horita, T.G. Langdon, Acta Mater. **50**, 553 (2002).
- [7] M. Oku, T. Shishido, Q. Sun, K. Nakajima, Y. Kawazoe, K. Wagatsuma, J. Alloys Comp. **358**, 264 (2003).
- [8] S. L. Shang, A. Saengdeejing, Z. G. Mei, D. E. Kim, H. Zhang, S. Ganeshan, Y. Wang, Z. K. Liu, Comput. Mater. Sci. **48**, 813(2010).
- [9] S. Ganeshan, S. L. Shang, H. Zhang, Y. Wang, M. Mantina, Z. K. Liu, Intermetallics **17**, 313 (2009).
- [10] W. Kohn, L. J. Sham, Phys. Rev. A. **140**, 1133 (1965).
- [11] <http://www.pwscf.org>.
- [12] H. J. Monkhorst, J. D. Pack, Phys. Rev. B **13**, 5188 (1976).
- [13] J. C. Schuster, J. Bauer, J. Less-Common Met. **109**, 345 (1985).
- [14] K. S. Kumar, Powder Diffr. **5**, 165 (1990).
- [15] U. Burkhardt, Y. Grin, M. Ellner, K. Peters, Acta Crystallogr. B **50**, 313 (1994).
- [16] F. A. Ainutdinov, S. K. Khairidinov, A. V. Vakhobov, Dokl. Akad. Nauk Tadzh. SSR **30**, 169 (1987).
- [17] T. Dagerhamn, Ark. Kemi **27**, 363 (1967).
- [18] P. B. Desch, R. B. Schwarz, P. Nash, J. Less-Common

- Met. **168**, 69 (1991).
- [19] H. Nowotny, C. E. Brukl, F. Benesovsky, *Monatsh. Chem.* **92**, 116 (1961).
- [20] K. B. Panda, K. S. R. Chandran, *Comput. Mater. Sci.* **35**, 134 (2006).
- [21] K. B. Panda, K. S. R. Chandran, *Acta Mater* **54**, 1641 (2006).
- [22] Y. H. Duan, Y. Sun, M. J. Peng, Z. Z. Guo, *Solid State Sci.* **13**, 455 (2011).
- [23] F. Y. Zhang, M. F. Yan, Y. You, C. S. Zhang, H. T. Chen, *Physica B* **408**, 68 (2013).
- [24] M. Jahnátek, M. Krajčí, J. Hafner, *Phys. Rev. B* **71**, 024101 (2005).
- [25] J. Wang, Central South University, Changsha, Hunan, China, 2012.
- [26] S. H. Liu, Central South University, Changsha, Hunan, China, 2010.
- [27] J. F. Nye, *Physical Properties of Crystals*, Oxford University Press, Oxford, 1985.
- [28] D. C. Wallace, *Thermodynamics of Crystal*, Wiley, New York, 1972.
- [29] O. Beckstein, J. E. Klepeis, G. L.W. Hart, O. Pankratov, *Phys. Rev. B* **63**, 134112 (2001).
- [30] W. Voigt, *Lehrbuch der Kristallphysik*, Teubner, Leipzig, 1928.
- [31] A. Reuss, *Z. Angew. Math. Mech.* **9**, 49 (1929).
- [32] R. Hill, *Proc. Phys. Soc. London* **65**, 349 (1952).
- [33] Y. H. Duan, B. Huang, Y. Sun, M. J. Peng, S. G. Zhou, *J. Alloys Compd.* **590**, 50 (2014).
- [34] S. F. Pugh, *Phil. Mag.*, **45**, 823 (1954).
- [35] J. J. Lewandowski, W. H. Wang, A. L. Greer, *Philos. Mag. Lett.* **85**, 77 (2005).
- [36] S. I. Ranganathan, M. Ostoja-Starzewski, *Phys. Rev. Lett.* **101**, 055504 (2008).
- [37] J. R. Rice, *J. Mech. Phys. Solids* **40**, 239 (1992).
- [38] V. Tvergaard, J. W. Hutchinson, *J. Am. Ceram. Soc.* **71**, 157 (1988).
- [39] J. F. Nye, *Physical Properties of Crystals*, 2nd ed., 20-24, Oxford, UK, Clarendon Press, 1964.
- [40] O. L. Anderson, *J. Phys. Chem. Solids*, **24**, 909 (1963).
- [41] E. Schreiber, O. L. Anderson, N. Soga, New York, McGraw-Hill, 1973.
- [42] W. C. Hu, Y. Liu, D. J. Li, X. Q. Zeng, C. S. Xu, *Comput. Mater. Sci.* **83**, 27 (2014).
- [43] M. A. Blanco, E. Francisco, V. Luana, *Comput. Phys. Commun.* **158**, 57 (2004).
- [44] <http://hyperphysics.phy-astr.gsu.edu/Hbase/Solids/phonon.html>.
- [45] M. E. Fine, L. D. Brown, H. L. Marcus, *Scr. Metall.* **18**, 951(1984).

---

\*Corresponding author: du511@163.com